Continental Shelf Research 28 (2008) 2371–2381

Contents lists available at ScienceDirect

Continental Shelf Research

journal homepage: www.elsevier.com/locate/csr

A simulation of the Chilean Coastal Current and associated topographic upwelling near Valparaíso, Chile

Christopher M. Aiken [a,b,*], Manuel I. Castillo [a], Sergio A. Navarrete [a]

[a] Estación Costera de Investigaciones Marinas, Center for Advanced Studies in Ecology and Biodiversity, Pontificia Universidad Católica de Chile, Casilla 114-D, Santiago, Chile
[b] Centro de Investigación en Ecosistemas de la Patagonia, Bilbao 449, Coyhaique, Chile

ARTICLE INFO

Article history:
Received 18 October 2007
Received in revised form
19 May 2008
Accepted 21 May 2008
Available online 6 June 2008

Keywords:
Coastal oceanography
Chile
Upwelling
Chile Coastal Current
Sea-surface temperature
Topographic eddies

ABSTRACT

A 4-year simulation of the surface circulation driven by the local wind on a section of the central Chilean coast is presented. The model is shown to reproduce the major observed features of the circulation. Comparison to observations of sea-surface temperature (SST) taken within the study area suggests that the model captures well coastal upwelling processes in the region. The circulation is shown to have two distinct modes corresponding to spring/summer and autumn/winter. During spring/summer sustained strong south-westerly wind forcing drives an equatorward coastal jet consistent with the Chile Coastal Current (CCC) and coastal upwelling at previously identified locations of intense upwelling at Topocalma Point and Curaumilla Point. Weaker winds during autumn/winter produce a slower CCC and a more homogenous SST field. Upwelling/relaxation and topographic eddies provide the main sources of variability on sub-seasonal time-scales in the model. The mechanisms responsible for each of these are discussed. Upwelling at Topocalma and Curaumilla Points is shown to be produced through generation of an upwelling Ekman bottom boundary layer following acceleration of the CCC close to the coast, reinforced by secondary circulation due to flow curvature around the headlands. Additional upwelling occurs north of Curaumilla Point due to development of shallow wind-driven overturning flow. Wind-sheltering is shown to be an important factor for explaining the fact that Valparaíso Bay is typically an upwelling shadow. Flow separation and eddy formation within Valparaíso Bay is seen to occur on the order of 10 times per year during relaxation after strong wind events and may persist for a number of weeks. Shorter lived topographic eddies are also seen to occur commonly at Topocalma and Toro Points. These eddies are shown to form in response to the surface elevation minima produced at each of these locations during upwelling.

1. Introduction

The Chile Coastal Current (CCC) is the coastal jet of the central south-east Pacific Ocean. Running in-shore of the Peru-Chile Current (also known as the Humbolt Current), the broad slow eastern boundary current of the south Pacific, the CCC is driven equatorward by persistent upwelling-favourable winds. Despite its proximity to the coast and its inferred importance in localised coastal upwelling (Johnson et al., 1980; Figueroa and Moffat, 2000) and larval transport (Aiken et al., 2007) the structure of the CCC remains relatively little studied. The CCC is known to respond quickly to local winds, reversing direction during relaxation after upwelling or during winter when northerlies become more common (Johnson et al., 1980; Pizarro et al., 1994; Narváez et al., 2006). In contrast, the other major currents of the region have received a considerable observational effort. The present state of knowledge of the regime of currents on the Pacific coast of South America is reviewed in Strub et al. (1998) and Halpin et al. (2004).

While upwelling-favourable winds and off-shore Ekman transport predominate along the central Chilean coast, the most significant upwelling tends to be associated with major geographical features of the coast (Strub et al., 1998). Figueroa and Moffat (2000) demonstrate that topographic effects are more important than the wind-driven off-shore Ekman flux in explaining the intensity of upwelling at a number of sites of regular upwelling along the Chilean coast. In the region of interest to this study, major sites of intense upwelling have been identified at Curaumilla Point (Johnson et al., 1980; Silva and Valdenegro, 2003) and Topocalma Point (Wieters et al., 2003; Narváez et al., 2004), and to a lesser extent at El Quisco (Poulin et al., 2002) (indicated by CM, TC and EQ, respectively, in Fig. 1). Of these, Curaumilla Point is observed to display the strongest and most persistent upwelling (Silva and Valdenegro, 2003). The cool water

* Corresponding author at: Estación Costera de Investigaciones Marinas, Osvaldo Mari'n 1672, Las Cruces, Chile. Tel: +56 35 431670; fax: +56 35 431720.
E-mail address: caiken@bio.puc.cl (C.M. Aiken).

0278-4343/$ - see front matter © 2008 Elsevier Ltd. All rights reserved.
doi:10.1016/j.csr.2008.05.006

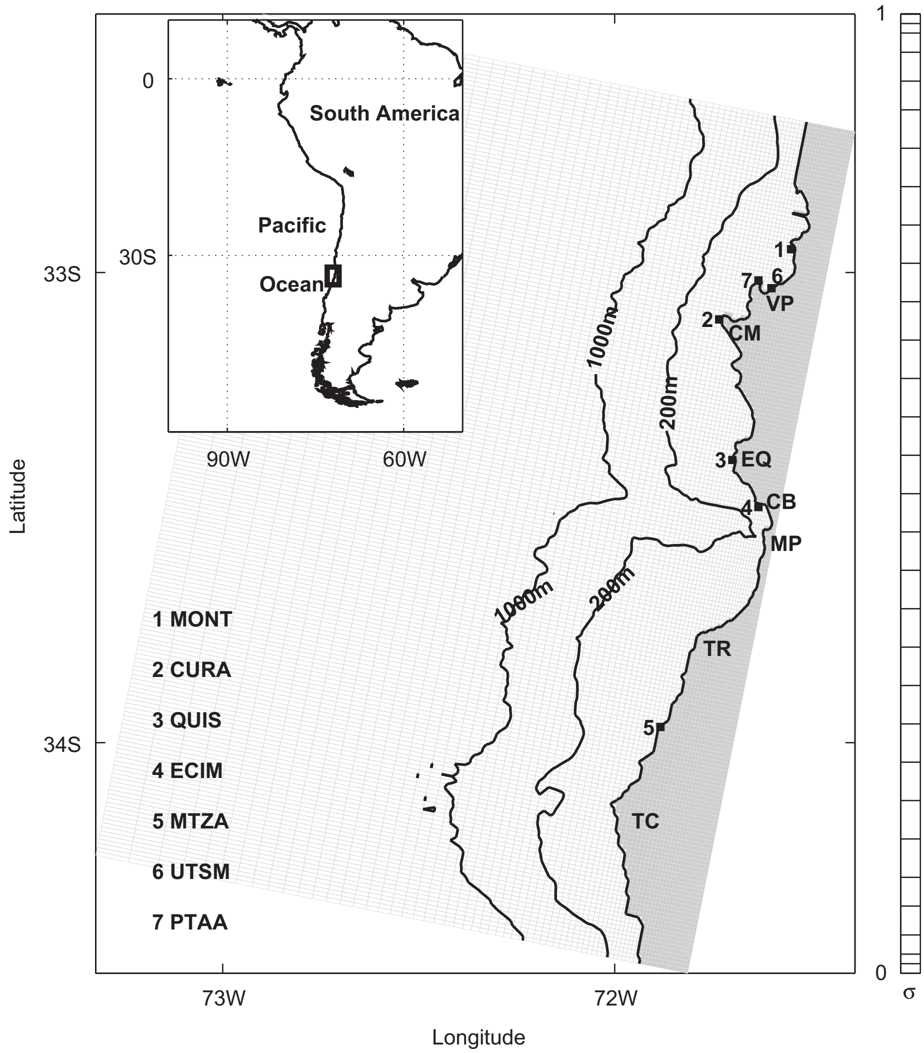

Fig. 1. Model grid, coastline and isobaths at 200 and 1000 m depths. Key locations are indicated: Valparaiso (VP), Curaumilla Point (CM), El Quisco (EQ), Cartagena Bay (CB), Maipo river mouth (MP), Toro Point (TR) and Topocalma Point (TC). Also shown numbered are the locations of observational records used in the study: Montemar (MONT), Curaumilla (CURA), El Quisco (QUIS), Las Cruces (ECIM), Matanzas (MTZA), Universidad Tecnica Federico Santa Maria (UTSM) and Punta Angeles (PTAA). Inset: The South American west coast with the region under study indicated by the box. The sigma levels used are indicated at right.

upwelled from these locations tends to be carried northwards along the coast and also off-shore in filaments (e.g. Silva and Valdenegro, 2003). Valparaíso and Cartagena Bays (indicated by VP and CB, respectively, in Fig. 1), however, tend to remain sheltered from the plumes of upwelled water (Sievers and Silva, 1979; Wieters et al., 2003; Narváez et al., 2004; Vargas et al., 2004; Lagos et al., 2005). The former, facing north and thus downstream from the upwelling site at Curaumilla Point, may be categorised as an upwelling shadow (Graham and Largier, 1997) and the latter, opening to the south, as an upwelling trap (Castilla et al., 2002). The sheltering of these locations is believed to have important biological implications (Castilla et al., 2002; Largier, 2002).

Prior to this paper, a number of studies have employed numerical models to investigate aspects of the coastal circulation in central Chile. Leth and Shaffer (2001) were able to reproduce many of the key features of the coastal circulation between 30°S and 45°S forcing an implementation of the Princeton Ocean Model (POM) with seasonal wind and thermal forcing. Leth and Middleton (2004) demonstrated that the generation of mesoscale meanders and eddies in the CCC may provide an important additional upwelling mechanism, and then extended their model to include a coastally trapped wave (CTW) paddle (Leth and Middleton, 2006). Middleton and Leth (2004) concentrated on the problem of spin-up and shut-down of coastal upwelling, using their model of the central Chilean coast as an example. Mesias et al. (2001, 2003) studied the dynamics of the upwelling circulation in Arauco Gulf at 37°S, emphasising the importance of flow separation from Lavapie Point. In the present study, we concentrate specifically on the character of the CCC and its role in topographic upwelling in a smaller geographical region than these earlier studies. This represents the first detailed simulation of the circulation in this region and the first effort to understand the mechanisms producing intense upwelling at Curaumilla Point.

The model used here simulates a component of the circulation driven by the local wind on the section of Chile's central coast between latitudes 32°S and 35°S (shown in Fig. 1). Despite being home to several commercially important fisheries and a number of large population centres, the oceanographic knowledge of this region remains limited. Based on a multi-year numerical simulation of the wind-driven flow in the region we investigate (1) the character of the seasonal cycle of the CCC in this region, and (2) the mechanisms controlling topographic upwelling along the coast. The model domain was centred on the Estación Costera de Investigaciones Marinas (ECIM), located in Las Cruces, where surveys of invertebrate recruitment patterns and oceanographic and meteorological conditions have been performed. Las Cruces, located within Cartagena Bay, is surrounded by a number of sites of regular intense upwelling, but is itself consistently within the Cartagena Bay upwelling trap. Details of the near-shore currents are of great importance for larval dispersal in this region (Largier, 2002; Aiken et al., 2007).

The paper is arranged as follows. Details of the model and 4-year simulation are presented in Section 2. The simulated circulation is discussed in Section 3, with particular attention to the seasonal cycle of the CCC and its role in topographic upwelling and eddy generation in the model. A conclusion is given in Section 4.

2. Model

The model used here was the Environmental Fluid Dynamics Code (EFDC; Hamrick, 1992). The EFDC solves the three-dimensional primitive equations with a free surface on a curvilinear grid in the horizontal and on sigma levels in the vertical. Temperature and salinity are prognostic and evolve through coupled transport equations. The system is closed with the Galperin et al. (1988) modification of the Mellor–Yamada level 2.5 turbulence scheme (Mellor and Yamada, 1982). Full details of the numerics and model physics are given in Hamrick (1992). The physics simulated by the model are essentially identical to those of other commonly used coastal ocean models such as the POM (Blumberg and Mellor, 1987). Major differences to the POM occur in the numerical solution of the governing equations, most notable of which being the use of a semi-explicit time-stepping scheme. The model is well-tested and has been previously applied successfully in a range of studies (e.g. Shen and Kuo, 1999; Hamrick and Mills, 2000; Yang and Hamrick, 2005).

The model domain (Fig. 1) covers the section of the Chilean central coast between approximately 32.5°S and 34.5°S, a distance of approximately 200 km, and extends 140 km off-shore. An orthogonal grid was used, rotated clockwise by 11.25° so as to follow the general orientation of the coast. This direction will be referred to hereafter as along-shore, and orthogonal to this as cross-shore. Along-shore grid spacing was constant at 1 km, while cross-shore grid spacing increased smoothly from 500 m next to the coast to 8 km at the off-shore edge of the domain. The resolution at the coast was adequate to represent the coastline and bathymetry accurately in shallow regions. An accurate representation of the bathymetry was found to be important for correctly reproducing certain features of the flow, such as the upwelling shadow in Cartagena Bay. The semi-implicit time-stepping scheme employed in EFDC greatly increased the allowable time-step for a given resolution relative to an explicit scheme, and hence facilitated the use of fine resolution in this study. EFDC uses a mode-splitting technique but with a single time-step, which in this case was 180 s.

Bathymetry for this region was determined by digitisation of the charts 4000 and 5000 of the Chilean Navy Hydrographic and Oceanographic Service (SHOA, Chile). The region's bathymetry is characterised by its extremely narrow shelf and the presence of a deep submarine canyon at the mouth of the Maipo River (MP in Fig. 1). Sigma-coordinate density-stratified ocean models typically develop spurious currents over such steep bathymetry, a result of round-off error in the calculation of the pressure gradient on sigma surfaces (e.g. Mellor et al., 1994; Shchepetkin and McWilliams, 2003). The problem was addressed in this study in the traditional manner—that is by smoothing the bathymetry to remove extreme gradients and through the use of relatively high horizontal resolution. Despite these measures, in the absence of external forcing currents of the order of 1 cm/s develop on the shelf and in the Maipo Canyon. However, as is commonly observed to occur in similar models, these currents do not develop once an external forcing was added, and in general are an order of magnitude less than the currents that develop under typical wind stress forcing. To reduce the allowable model time-step bathymetry was cropped at 1000 m depth. A total of 31 sigma layers were used, concentrated at the surface and bottom so as to maximise resolution of the respective boundary layers (see Fig. 1).

Boundary conditions at the along-shore ends of the numerical domain were periodic in all variables. A 15 km buffer region was added to each end of the model grid in which the bathymetry was linearly interpolated to provide a smooth transition across the periodic boundary. A periodic treatment of along-shore boundaries provides an extremely robust model, and as such is a commonly used solution to the open boundary problem in the study of circulation in regions with relatively straight coastlines, such as is the case here (e.g. Oke et al., 2002). This choice of boundary conditions has a number of limitations, however, that should be noted in the interpretation of the results, primarily that the use of periodic boundaries prevents the model from being able to sustain net along-shore pressure gradients. (It may be noted, however, that local along-shore pressure gradients are supported in the model.) Consistent with the periodic boundaries an f-plane approximation is used with $f = -8 \times 10^{-5}$. A condition of no normal flow was imposed at the off-shore boundary.

The inability of the model to sustain net along-shore pressure gradients is a factor that inhibits the formation of a Poleward Undercurrent (PUC) in the model. It is possible that the use of an f-plane also inhibits undercurrent formation (Philander and Yoon, 1982; Suginohara and Kitamura, 1984). Poleward undercurrents are ubiquitous features of the Chilean coastal circulation and of eastern boundary regions in general (Fonseca, 1989; Neshyba et al., 1989). However, given that their adequate simulation in numerical models has proven difficult, in particular in limited area models with synoptic scale wind forcing (see Leth and Middleton, 2004), in the present study we chose to ignore effects of the PUC upon the CCC. Clearly, the presence of a PUC would have consequences for the nature of the CCC, potentially increasing baroclinicity and hence the development of meanders and eddies. However, the fact that the sensitivity of the numerical simulations of Leth and Middleton (2004) to details of the PUC that was enforced in their model was relatively small, it is likely that the consequences of the PUC for the CCC is of secondary importance. The effect of the PUC upon the CCC in this region is a topic of future research. The periodic boundaries also may have a secondary influence upon the degree of upwelling produced in the model. While a net along-shore pressure gradient is absent during the initial stages after application of an upwelling-favourable wind such that upwelling would be expected to proceed as simulated in the model, arrival of CTWs from the wind field's origin would be expected to shut-down the upwelling (e.g. Philander and Yoon, 1982; Middleton and Leth, 2004). As CTWs are clearly not produced at the model's upstream boundary, this upwelling shut-down process cannot occur. However, as the typical time-scale for upwelling-favourable wind events as simulated in the model is less than the time required for arrival of the first CTW mode, this effect is likely to be minor.

The model was forced predominantly by application of a time-dependent surface wind stress, and to a lesser degree through relaxation to the climatological density profile, as discussed below. Daily wind stresses were derived from wind velocity recorded at the ECIM in Las Cruces, and then interpolated linearly to the model time-step. Winds in this region are upwelling-favourable for much of the year, in particular in austral spring and summer, while downwelling-favourable winds generally only occur during the austral winter, corresponding to the passage of atmospheric fronts and their associated strong northerlies (Narváez et al., 2004). The wind observations are discussed in detail by Kaplan et al. (2003) and Narváez et al. (2004, 2006). As discussed in those studies, open ocean wind speed was estimated by taking the daily mean of the coastal wind over the period 1–5 p.m. each day. It has been shown (Castillo and Largier, unpublished manuscript) that the ECIM mean wind calculated in this way correlates well with scatterometer estimates of the open-ocean wind immediately adjacent to Las Cruces. This afternoon average wind was used for calculating the spatially homogeneous wind stress field used to drive the model.

Given the predominance of on-shore winds and the relatively straight coastline, the assumption of homogeneity of the wind field is believed to be valid to leading order for most of the model domain. Valparaíso Bay, however, is commonly noted to be the only location on this section of coast that is significantly sheltered from the prevailing south-westerlies. Thus, an exception to spatial homogeneity of the wind field used to drive the model was applied within Valparaíso Bay. A simple model of wind-sheltering in the bay was used in which the wind stress was reduced linearly to zero as a function of distance from the south-east corner of the bay whenever the applied wind had a component from the south. This treatment of the wind field within Valparaíso Bay was found to substantially improve the model's recreation of the upwelling shadow there, suggesting that this sheltering plays an important role in determining the circulation within the bay.

To provide quantitative support for the occurrence of wind-sheltering within Valparaíso Bay, an analysis was performed of winds recorded within the bay at the Universidad Técnica Federico Santa Maria (UTSM—33°02′S, 71°36′W) and at Angeles Point (PTAA—33°01′S, 71°38′W). UTSM is located approximately 5 km north from the southern corner of the bay, and thus is moderately sheltered to the south, while PTAA lies relatively exposed at the tip of the headland that encloses Valparaíso Bay (see Fig. 1). As for the ECIM winds, daily mean winds over the period 1–5 p.m. were calculated at each location. It was found that for days with south-westerly winds at ECIM, the mean wind speed at ECIM (3.8 m/s) was slightly less than that at PTAA (4.3 m/s) but over twice that at UTSM (1.7 m/s). This confirms the relative weakness of south-westerlies at Valparaíso, and suggests that the weakening is indeed restricted to within the bay, as represented in the wind field used to drive the model.

The three-dimensional temperature and salinity fields were initialised to monthly-mean climatological values taken from the NODC Levitus World Ocean Atlas, 1998 for the location (33°S, 72°W). Temperature and salinity were then continually relaxed towards the appropriate month's climatology via Newtonian damping with a relaxation time-scale τ of 15 days, according to

$$X = X + \frac{X^{*} - X}{t},$$

where X represents the modelled temperature or salinity and X^{*} the climatological value.

The Levitus data were provided by the NOAA-CIRES Climate Diagnostics Center, Boulder, CO, USA, from their Web site at: ⟨http://www.cdc.noaa.gov/⟩. The relaxation time-scale τ was reduced linearly towards a value of 5 days over the width of the periodic buffer zones, in order to provide some damping of baroclinic structures re-entering the domain through the periodic boundary. Velocity and sea surface elevation were initialised to zero and the model spun-up for 30 days using the observed ECIM winds corresponding to November 1999. The model was then integrated forward for 1490 days, corresponding to the period December 1, 1999–January 1, 2004.

3. Results

3.1. Model-observation comparisons

In this section we assess the ability of the model to reproduce empirical observations taken within the modelled region. While a number of potentially significant external forces have not been included in the model, including spatial variability in the wind field, CTWs and explicit thermal forcing, we show here that the model is able to reproduce a significant proportion of the sea-surface temperature (SST) variability in this region over synoptic time-scales. Narváez et al. (2004, 2006) demonstrated that forcing by the local wind is strongly and significantly correlated ($r = 0.47$, $p < 0.05$) to SST variability in this region. A comparison of SST in the model to that recorded *in situ* at ca. 1 m depth at a number of locations (see Narváez et al., 2006 for details) covered by the model domain for period 2001–2003 is given in Table 1, while a portion of the time-series is displayed in Fig. 2. For the comparison, both the modelled and observed data were daily-averaged and high-pass filtered with a cut-off frequency of $(60\,\text{days})^{-1}$. Correlations between the filtered time-series were calculated for the spring/summer and autumn/winter of each year. All correlations given in Table 1 are significant, with $p < 0.01$.

The correlations vary considerably between individual locations and seasons, but in general all are greater than 0.3. As may be appreciated in Fig. 2, while the model is quite successful at reproducing reductions in SST associated with wind-driven upwelling, SST increases are not well reproduced, as may be expected from the model's lack of any realistic physical heating mechanisms. Nonetheless, the model and observations are reasonably well correlated, particularly at CURA and QUIS, locations associated with intense upwelling. The fact that model performance is worst at ECIM likely stems from the fact that it is located in an upwelling shadow, where upwelling-induced SST variability is less pronounced.

In summary, despite not including a number of important mechanisms that drive SST variability, the model has proven capable of reproducing a significant proportion of the observed SST signal along the coast, and thus is believed to reproduce the circulation in the region to a reasonable degree, in particular the upwelling circulation.

Direct observations of the ocean velocity field in the area are few and in general of short duration and close to shore (Narváez et

Table 1
Correlation coefficients between modelled and observed SST anomalies (after removal of mean and seasonal cycle) from various locations within the model domain (see Fig. 1)

Year	Season	MONT	CURA	QUIS	ECIM	MTZA
2001	SUM	–	0.52	–	0.35	0.48
	WIN	–	0.52	–	0.54	0.55
2002	SUM	0.46	0.51	0.57	0.30	0.35
	WIN	0.42	0.63	0.59	0.54	0.52
2003	SUM	0.71	0.61	0.47	0.36	0.28
	WIN	0.33	0.42	0.54	0.39	0.35
ALL	SUM	0.53	0.49	0.48	0.32	0.36
	WIN	0.35	0.46	0.50	0.44	0.46
ALL		0.44	0.45	0.48	0.36	0.38

Correlations are shown for individual 6-month periods each year corresponding to September–February (SUM) and March–August (WIN), as well as for the entire simulation (ALL).

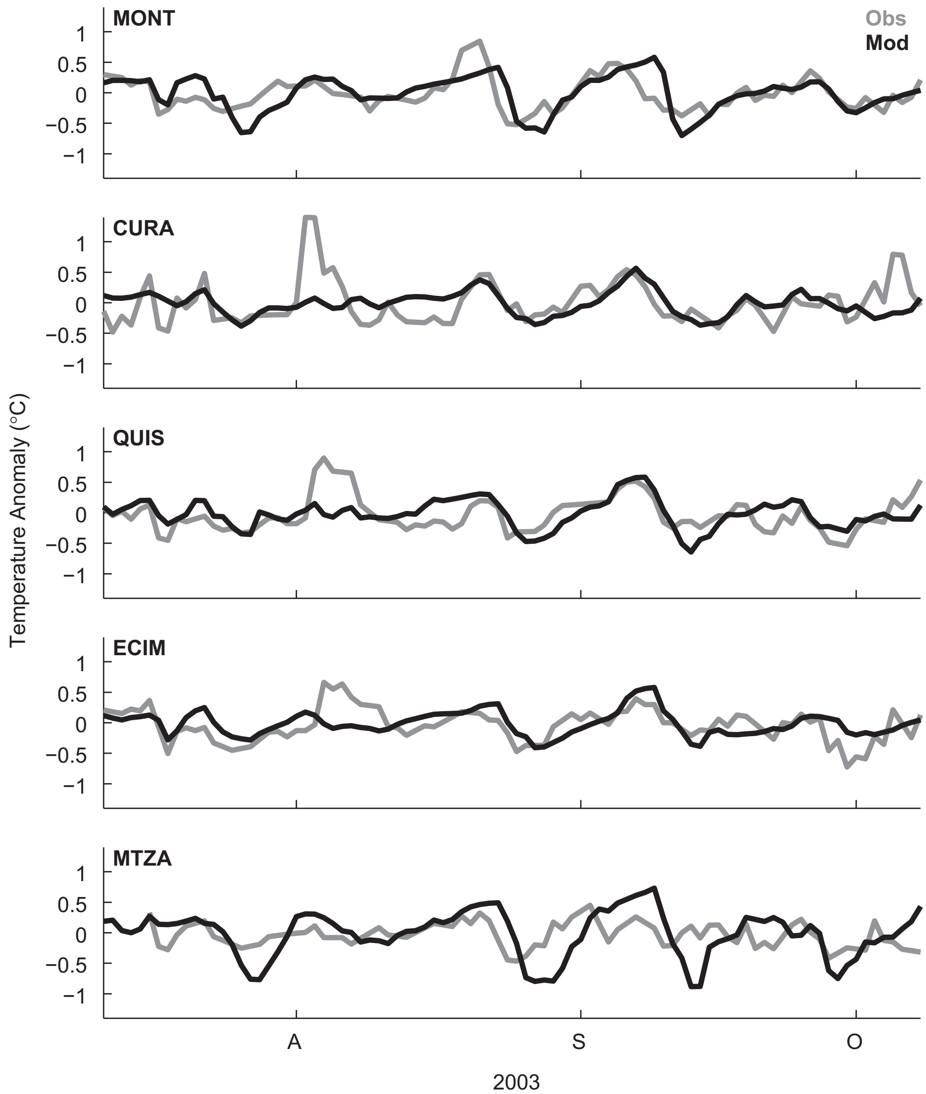

Fig. 2. Time-series of modelled (dark) and observed (grey) SST anomalies (after removal and mean and seasonal cycle) at Montemar (MONT), Curaumilla (CURA), El Quisco (QUIS), Las Cruces (ECIM) and Matanzas (MTZA).

al., 2006; Piñones et al., 2005; Vargas et al., 2004; Navarrete, unpublished manuscript). The longest time-series comes from Narváez et al. (2006), who measured the near-surface ocean velocity close to shore within Cartagena Bay over the period June 2001–February 2003. These measurements are in general agreement with the velocity field simulated in the model: the observed daily-averaged near-shore velocity was found to be weakly northwesterly (mean 0.2 cm/s) but variable (standard deviation 2 cm/s), while at the same location the model simulates a stronger northwesterly flow of 0.64 cm/s with a standard deviation of 2.58 cm/s.

Further indirect support for the success of the model in reproducing the surface circulation comes from the good agreement found between the patterns of settlement predicted by simulating passive larval dispersal using the model (Aiken et al., 2007) and those for intertidal barnacles observed in the region (Lagos et al., 2005).

3.2. Character and seasonality of the modelled CCC

While the relative success of the model in reproducing the velocity field within Cartagena Bay and the timing and location of upwelling events is encouraging, unfortunately no observations exist to indicate details of the more energetic part of the circulation, in particular the off-shore position, structure and intensity of the CCC within the modelled area. As a result, the model results provide a first estimate of the character of the CCC in this region.

The CCC was represented in the model as a surface intensified coastal jet positioned above the shelf break and/or directly adjacent to the coast. Fig. 3a and b depicts the simulated surface velocity field averaged over summer (panel a) and winter (panel b), demonstrating the marked seasonality in the strength of the modelled CCC. In general, the CCC reached its maximum speeds during spring, corresponding to the spring maximum in northwards wind stress, and was slowest during winter, occasionally reversing direction following the strong northerly winds associated with winter storms. Thus, the transition between late winter and early spring represented the time of most rapid change in the character of the modelled CCC. Maximum annual mean speeds of 27 and 23 cm/s, respectively, occurred at the surface where the CCC passed close to Curaumilla and Topocalma Points (indicated by CM and TC, respectively, in Fig. 1), although peak speeds of up to 80 cm/s occurred during spring at both locations.

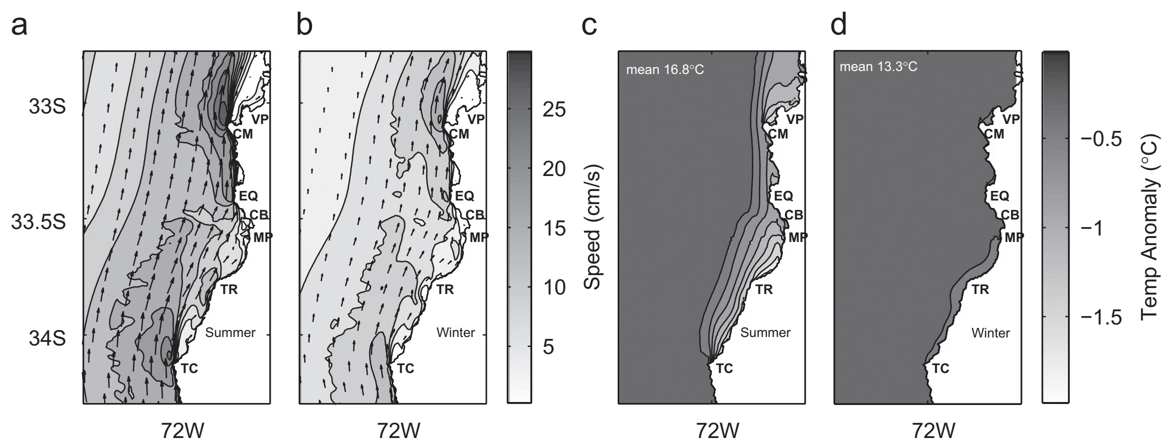

Fig. 3. Mean surface velocity and surface temperature anomalies for the seasons of Summer (December–February) and Winter (June–August). In (a) and (b), velocities are denoted by vectors, while speed is contoured with a contour interval of 1 cm/s. For clarity only a subset of model velocities are shown as vectors. The contour interval in (c) and (d) is 0.2 °C. The mean surface temperature for each season is indicated in the upper left corner of (c) and (d).

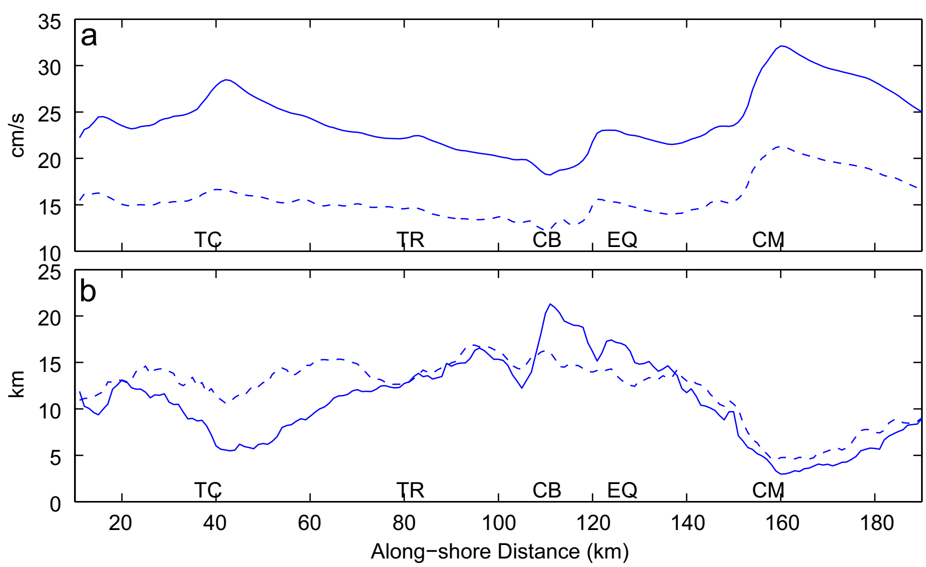

Fig. 4. Mean speed (a) and standard deviation of the off-shore distance (b) of the CCC as a function of along-shore distance during spring/summer (September–February, solid) and autumn/winter (March–August, dashed). Locations of key features are indicated at bottom using the abbreviations of Fig. 1.

In between Topocalma and Curaumilla Points the CCC was slower and less distinct. As observed by Narváez et al. (2006), in-shore of the CCC currents were generally weak and variable.

In order to quantify the path of the CCC and examine its variability throughout the simulation, the distance off-shore of the surface velocity maximum at each along-shore row of the numerical domain was determined. Fig. 4 presents the mean maximum speed (panel a) and standard deviation in the off-shore distance of the core of the CCC (panel b) as a function of distance along-shore. While the speed of the CCC was strongest next to the Topocalma and Curaumilla headlands, its off-shore position varied relatively little at these locations, especially in the latter case. The tendency for the CCC to remain close to these headlands is true at Topocalma only for spring/summer, but occurs throughout the year at Curaumilla. Conversely, the mean flow of the CCC is weakest, and variability in the location of its core greatest, off-shore of Cartagena Bay. As will be discussed further below, the fact that the CCC appears to be strongly constrained to pass close to Curaumilla and Topocalma Points may help explain the consistency of intense upwelling observed at these locations.

While annual mean surface velocities were northwards for the majority of the water column, mean poleward surface flow occurred consistently on the eastern side of Valparaíso Bay. In this case, the predominance of southward flow, despite the prevailing south-westerly winds, is associated with regular eddy formation in the lee of headlands to the south, discussed below. Weak mean poleward flow is also seen at some locations along the shelf break, generally within the bottom boundary layer at depths greater than 500 m.

The strong seasonality of the local wind forcing is also reflected in the seasonally averaged anomalous SST fields (Fig. 3c and d). Substantial outcropping of isotherms is seen during spring and summer, corresponding to the maximum in the strength of the south-westerly winds. The largest negative temperature anomalies were found at Laguna Verde Bay in the northern lee of Curaumilla Point, along the stretch of coast north from Topocalma and Toro Points, and north of El Quisco. All these locations have been identified with regular intense upwelling from satellite and *in situ* observations (Narváez et al., 2004; Wieters et al., 2003). The tendency for SST in Cartagena and Valparaíso Bays to be warmer than locations immediately upstream can also be seen, consistent with them being upwelling shadows. As mentioned previously, and discussed more fully below, successful simulation of the temperature structure in Valparaíso Bay required special treatment of the wind field there. The homogeneity in SST simulated during autumn and winter indicates the almost complete absence of upwelling, associated with the weaker and more variable winds and reduced strength of the CCC.

3.3. Upwelling mechanisms

The relative success of the model in reproducing the locations and timing of intense upwelling suggests that it can be used to investigate the mechanisms responsible for upwelling in the real system. To this end, we analyse a typical upwelling event that occurred during April 2003. For a number of weeks prior to the upwelling event, weak south-westerly winds of less than 3 m/s persisted. Between April 23 and 24, the wind turned to the south and increased to over 12 m/s before returning rapidly to the original weak south-westerly conditions from April 25 onwards. We discuss below the evolution of the upwelling circulation at Topocalma and Curaumilla Points as simulated in the model, and compare this to the case at the prominent shadow zone at Valparaíso Bay.

3.3.1. Topocalma Point

Fig. 5 shows the off-shore circulation and temperature structure in a cross-shore section at Topocalma Point on April 21, 24 and 30, 2003. These dates correspond to the pre-, peak- and post-upwelling conditions, respectively. Prior to the upwelling event, the CCC ran weakly above an equally weak return flow centred at 50 m depth. Application of the strong upwelling-favourable winds produced off-shore velocities up to 10 cm/s in a 20 m thick surface Ekman layer, while the CCC broadened, deepened and accelerated northward. The deepening and intensification of the CCC resulted in strong northwards velocities adjacent to the ocean floor down to depths of over 50 m. Through standard Ekman dynamics (e.g. Oke and Middleton, 2000) the resultant southward bottom stress generated an upwelling bottom boundary layer (BBL) which was fed by on-shore flow close to the bottom at depths to 100 m. Upwelling in the BBL was sufficient to raise isotherms by up to 50 m during April 24 off the headland, although little change is seen in surface temperature. Due to advection, surface outcropping of isotherms occurs downstream of the site of strong upwelling. Following weakening of the wind the CCC slowed and shallowed, reducing the bottom stress and shutting down the BBL.

When a flow is forced to round a headland, a vertical imbalance in the centrifugal acceleration due to bottom friction

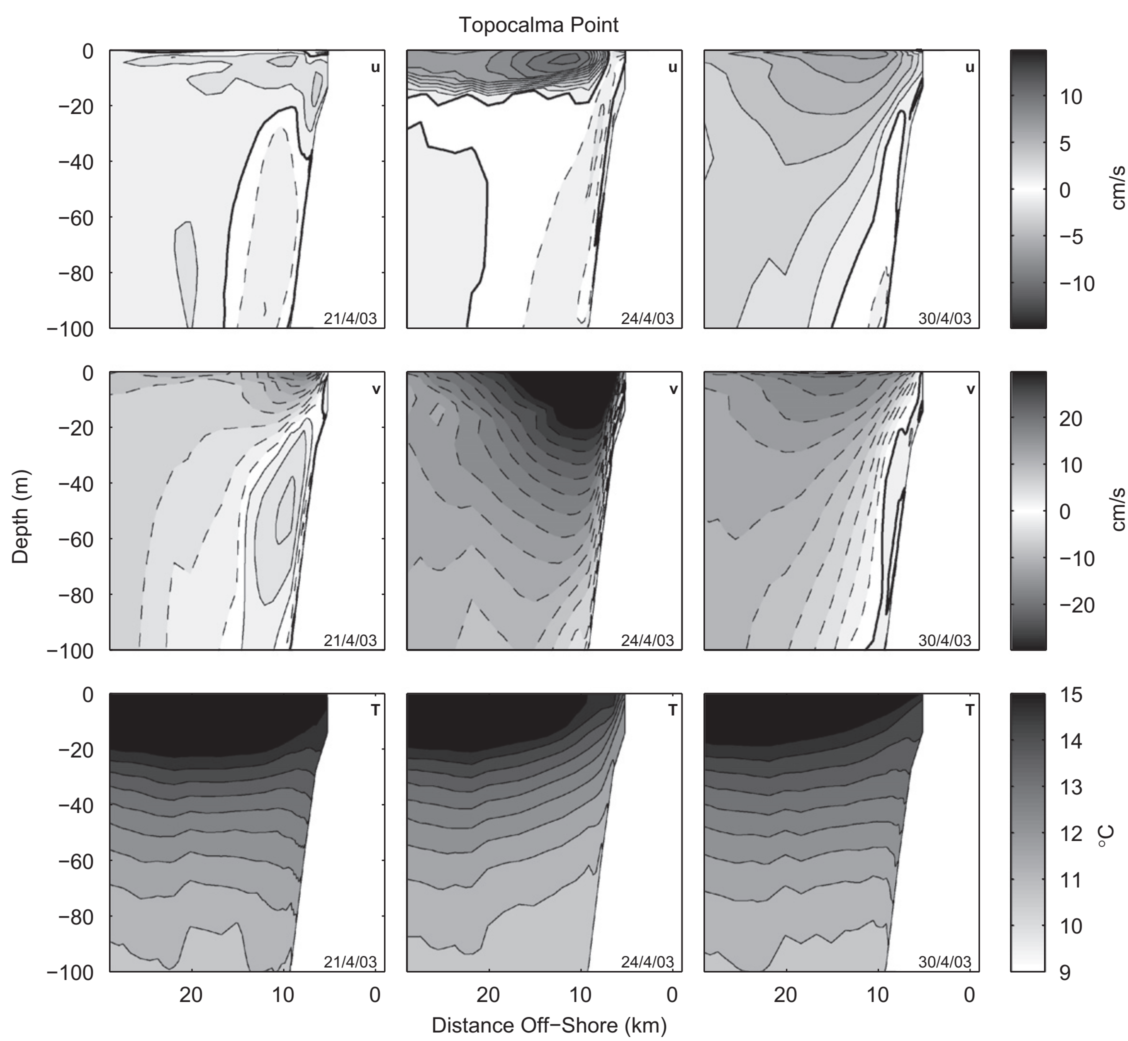

Fig. 5. Cross-shore transect at Topocalma Point of cross-shore velocity (u), along-shore velocity (v) and temperature (T) for the period April 21–30, 2003. For u the contour interval is 1 cm/s, solid/dashed contours represent off-shore/on-shore velocities. For v the contour interval is 2 cm/s, solid/dashed contours represent southwards/northwards velocities. In both cases the zero contour is darker. The contour interval for temperature is 0.5 °C.

may produce a circulation transverse to the direction of flow, known as a secondary circulation (e.g. Kalkwijk and Booij, 1986). The ratio of the importance of flow curvature to rotational effects in driving transverse velocities may be estimated through calculation of a modified Rossby number $R_{om} = \gamma U_s/|f|R_s$, where $\gamma = (1 - \hat{U}^2/U_s^2)/(1 - \hat{U}/U_s)$, $\hat{U}$ is the vertically averaged streamwise velocity, U_s is the surface streamwise velocity, f is the Coriolis parameter and R_s is the radius of curvature of the streamline (Alaee et al., 2004). For flow rounding Topocalma Point at the peak of the upwelling event, $\hat{U}\sim 25\,\mathrm{cm/s}$, $U_s\sim 50\,\mathrm{cm/s}$, $\hat{U}^2\sim 900\,\mathrm{cm^2/s^2}$ and $R_s\sim 13\,\mathrm{km}$, yielding $R_{om}\sim 0.6$. This suggests that flow curvature also plays a significant role in driving transverse velocities and hence upwelling. Importantly, the sense of flow curvature is such that the secondary circulation would reinforce the onshore bottom Ekman transport, thus strengthening the upwelling.

An additional factor favouring upwelling at Topocalma was the fact that, as noted in Section 3.2, the CCC remained close to the headland throughout the spring–summer peak upwelling season, such that intensification of the CCC due to strong southerly or south-westerly winds could commonly produce strong bottom stresses adjacent to the headland.

3.3.2. Curaumilla Point

The upwelling circulation simulated off-shore of Curaumilla Point (Fig. 6) exhibits similarities to that at Topocalma, but is complicated by the presence of Laguna Verde Bay to the north. As at Topocalma, intensification of the south-westerly winds caused the CCC to strengthen, broaden and deepen, producing strong northwards velocities immediately next to the western edge of the headland and hence driving an upwelling BBL. This process raised isotherms at the western edge of Laguna Verde Bay at a similar rate to that seen at Topocalma. For the flow rounding Curaumilla Point at the peak of the upwelling event the modified Rossby number $R_{om}\sim 0.5$, suggesting that secondary circulation also made an important contribution to the upwelling circulation.

Within Laguna Verde Bay the increased winds also produced a weak shallow northwards flow at the surface. The resulting flow divergence at the northern edge of the headland was compensated by a deeper southwards return flow, which drove further upwelling at the northern edge of the headland. The combination of the BBL flow, secondary circulation and shallow overturning flow within the bay may explain the greater intensity of upwelling observed at Curaumilla Point compared to that elsewhere on this section of coast. In addition, as noted for Topocalma Point, the fact

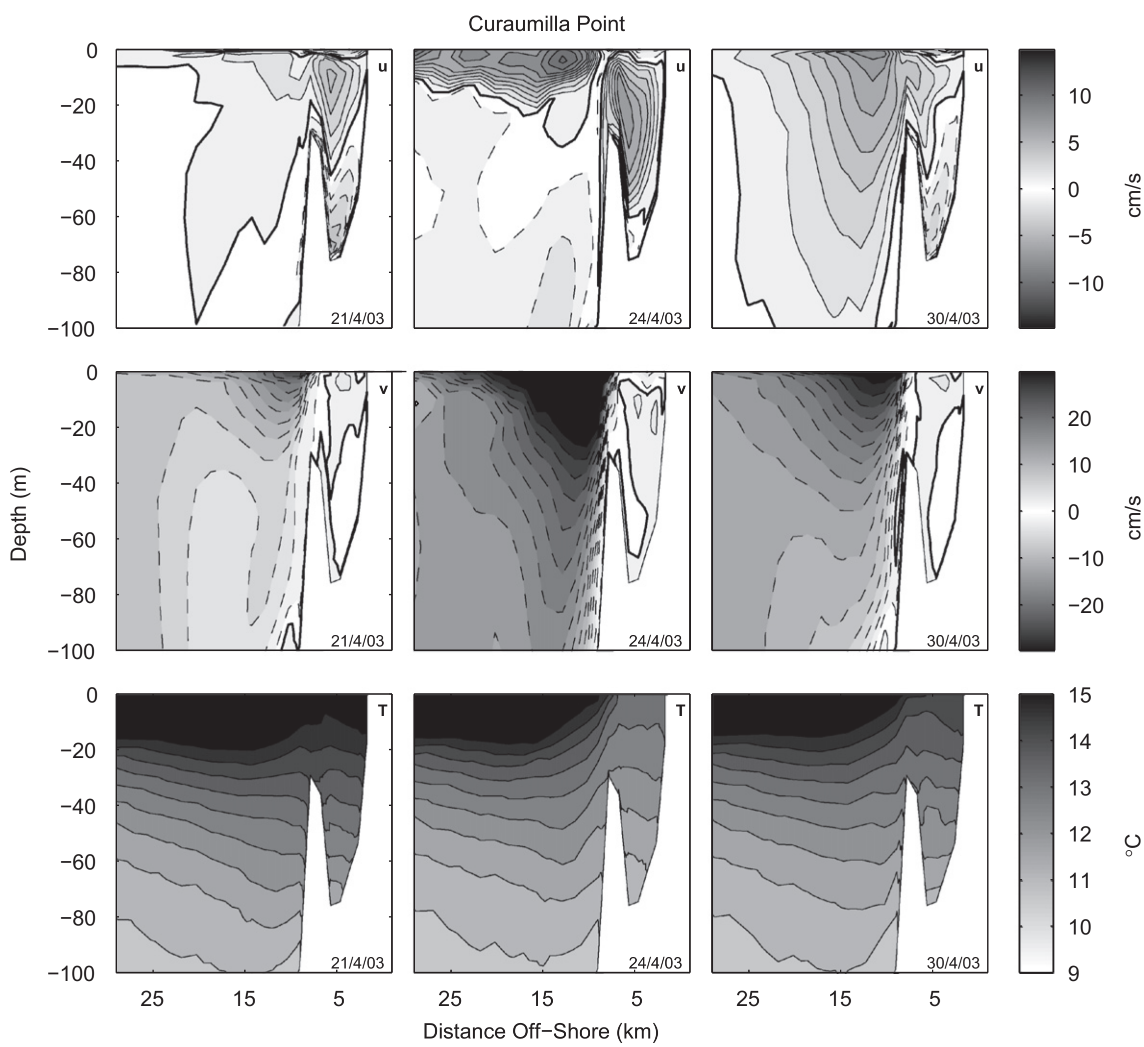

Fig. 6. As in Fig. 5 but for Curaumilla Point (CM).

that the CCC appears to be constrained to remain close to the headland suggests that intensification of the CCC will in general be accompanied by strong bottom stresses and a resultant upwelling circulation at the headland.

3.3.3. Valparaíso Bay

The model response in Valparaíiso Bay during the upwelling event is pictured in Fig. 7. Although geometrically similar to the Curaumilla Point/Laguna Verde Bay system, Valparaíso Bay is known to be an upwelling shadow, with consistently warmer surface temperatures than in nearby Laguna Verde Bay during upwelling events (Silva and Valdenegro, 2003; Narváez et al., 2006). We find that the distinct character of the two locations is due to differences in the position of the CCC and the mode of recirculation within the bays. In contrast to Curaumilla Point, the core of the CCC resided too far off-shore to produce a significant southwards bottom stress on the seaward side of Angeles Point—the headland that closes Valparaíso Bay to the west—and hence an upwelling BBL did not form there. Similarly, the relative weakness of flow adjacent to the headland meant that flow curvature effects were insignificant. The wind-driven surface Ekman layer formed away from the coast, off-shore from the core of the CCC, while the flow next to Angeles Point at the western end of the bay was onshore throughout the water column. As a result, little upwelling was driven at Angeles Point, and much of the uplift of isotherms seen was in fact due to upwelling from Curaumilla further south.

The response of the flow to the strong wind forcing within Valparaíso Bay is also distinct from that in Laguna Verde Bay. Prior to the sudden increase in wind stress, the flow in both bays was similar. However, following intensification of the wind and development of northwards velocities at the surface, weak southwards flow persisted at the eastern edge of Valparaíso Bay, indicating the existence of a horizontal recirculation within the bay. This differs from the situation within Laguna Verde Bay, where shallow overturning flow occurred.

The development of a horizontal rather than vertical cell was aided by the wind-sheltering experienced by Valparaíso Bay. In experiments in which a spatially constant wind stress was used inside the bay (results not shown), northwards flow was driven at the surface throughout the bay, requiring upwelling against the coast to balance mass, similar to the situation in Laguna Verde Bay. As will be discussed below, the fact that upwelling is limited to Laguna Verde Bay generates a horizontal pressure gradient between the two bays that further drives horizontal recirculation in Valparaíso. The recirculating flow also acts to slow entrainment of water recently upwelled from Curaumilla Point into the bay, further increasing the surface temperature difference between these two locations.

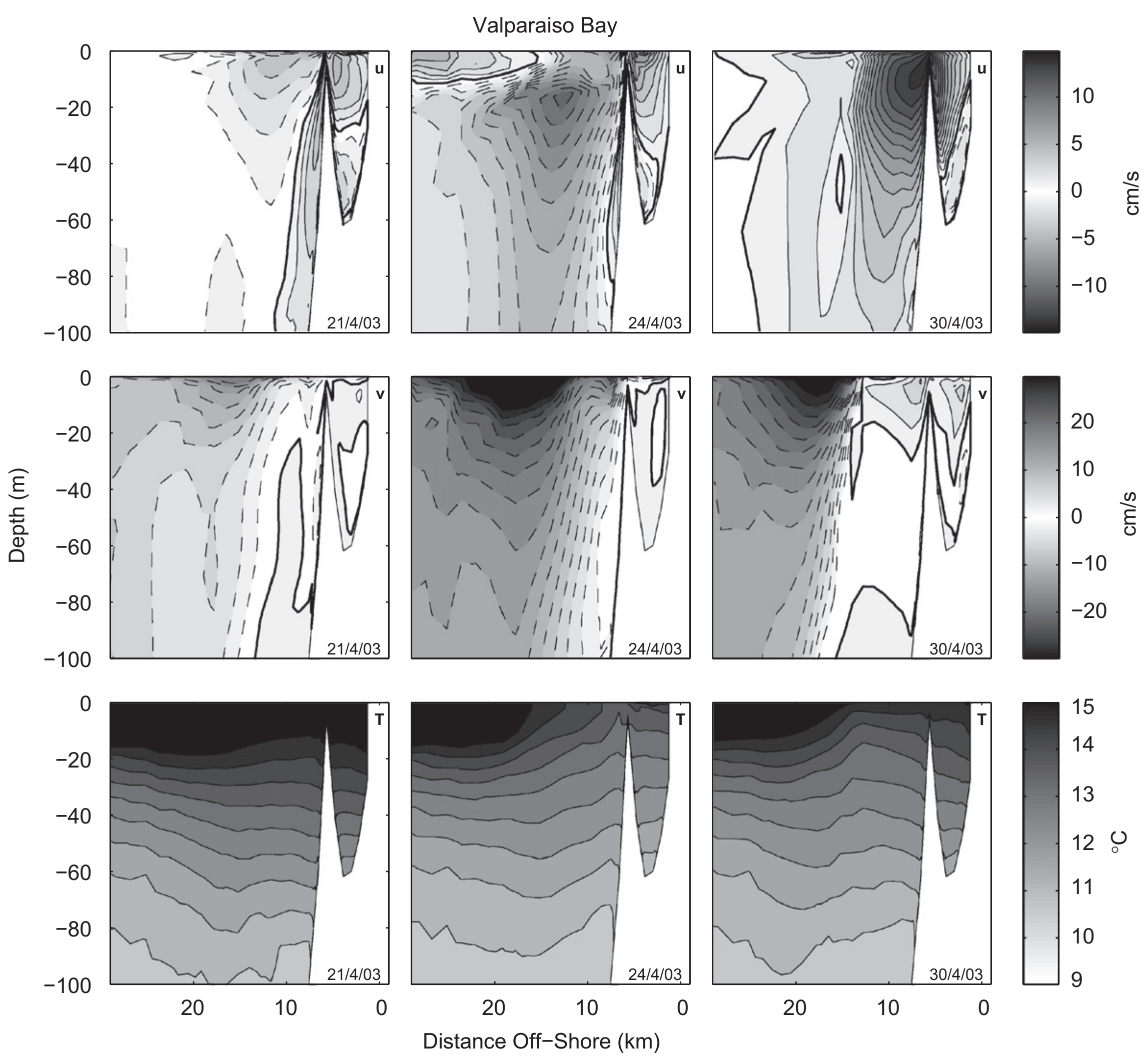

Fig. 7. As in Fig. 5 but for Valparaiso Bay (VP).

3.4. Topographic eddies

In the model topographically induced eddies occurred commonly in the lee of the Topocalma, Toro and Curaumilla Points. In general, favourable conditions for eddy generation occurred when strong southerly winds, usually also associated with coastal upwelling, were followed by a period of weaker winds that persisted for a number of days. Once detached from the headland, the Topocalma and Toro eddies were carried northwards in the mean flow and dissipated relatively rapidly, surviving only on the order of days. The Curaumilla eddy dissipated more slowly—over time-scales of weeks—and would commonly remain in the Valparaíso vicinity for up to a month. In all cases, however, the eddies were dissipated rapidly by strong wind events. Thus, while topographic eddy formation occurred between spring and autumn, eddies were most likely to be found in the simulation during the summer, when upwelling occurred regularly but dissipative strong wind events were less common. Eddies were generated relatively commonly during spring, but tended to exist for short periods due to the greater prevalence of strong winds.

The mechanism responsible for generation of the eddies is essentially the same in each location. A typical eddy formation event that began on March 29, 2000 is depicted in Fig. 8 for Curaumilla Point. During the initial strong southerly winds surface flow was uniformly toward the north. The upwelling circulation resulted in negative surface elevation anomalies at the coast, in particular in the location of intense upwelling situated along the northern shore of the headland. Thus, the upwelling event was accompanied by the development of along-shore variability in the sea surface elevation field, and hence by the generation of along-shore barotropic pressure gradients. Upon removal of the wind stress the flow responded geostrophically to the resulting pressure field, following the contours of surface elevation. At the coast, however, where geostrophic flow is not possible due to the solid barrier, the pressure gradient was balanced by the tendency, thus generating a current along the coast directly down the pressure gradient. Establishment of this upstream coastal current accompanied the corresponding adjustment of the pressure field such that a geostrophically balanced eddy was formed. Although originating within Laguna Verde Bay, the eddy was carried downstream in the mean flow to lie off Valparaiso Bay soon after formation.

This mechanism is distinct from that typically associated with wake formation in the lee of headlands, where eddy formation occurs when the incident flow surpasses a critical Reynolds number and separates from the headland tip (e.g. Aiken et al., 2003). Eddy formation in the model differs from the standard two-dimensional description because of the fact that the modelled flow is forced directly by the wind. The strength of the CCC and the shape of the headlands is such that, in the absence of local wind forcing, the flow would be expected to be continuously separated from the headlands, especially so for Curaumilla Point. Eddies were not constantly observed, however, because the wind drove northwards flow in the lee of each headland, with the notable exception of Valparaíso Bay. In addition to transferring momentum directly to the flow field, variability in the surface elevation field due to the wind forcing was seen to be a vital factor for explaining the eddy formation.

While none of these eddies have been directly observed, the observations of Johnson et al. (1980) are consistent with the occurrence of the Curaumilla/Valparaíso eddy. They found that cyclonic flow established in the lee of the Curaumilla Point during weak winds following an upwelling event, as is seen to occur in the model. The eddies generated in the model are also broadly consistent with the study of Valle-Levinson and Moraga-Opazo (2006), who also observed clockwise eddies in the lower portion of two other equatorward facing bays in northern Chile. In their case, two counter-rotating eddies occurred within each bay, a result they concluded was linked to the fact that bay lengths were over twice the radius of curvature of the upstream headlands. As the radius of curvature of Curaumilla Point is less than twice the length of Laguna Verde Bay, their analysis would suggest the formation of single eddy, as indeed produced in the model.

If the eddies simulated in the model do indeed occur in the real system, this may have a number of important biological implications for the area. As their generation generally follows an upwelling event, the eddies tend to trap cold upwelled waters in their centres. In addition, their cyclonic sense of rotation results in further Ekman pumping at the eddy centre. As a result, the eddy centres represent patches of biologically highly productive water that can persist in a single location for a number of days or weeks. The eddies, in particular that at Curaumilla, also would provide a potential mechanism for larval retention. Under normal conditions larvae passing Punta Curaumilla are likely to be carried far to the north. However, the presence of the eddy may provide a pathway for larvae to be retained in the region and ultimately to reach the coast. The characteristics of larval dispersal in the model are discussed in Aiken et al. (2007).

4. Conclusion

Despite the use of idealised boundary conditions that do not permit the development of a PUC, the model presented here proved to be capable of simulating a number of the surface features observed in the region. The dominant feature of the simulations was a surface intensified coastal current consistent with the CCC. The CCC was present almost constantly in the simulation, disappearing or reversing only briefly during winter northerly wind events. The three major upwelling centres located within the model domain were well represented as determined by comparison to coastal observations of SST. Intense upwelling at

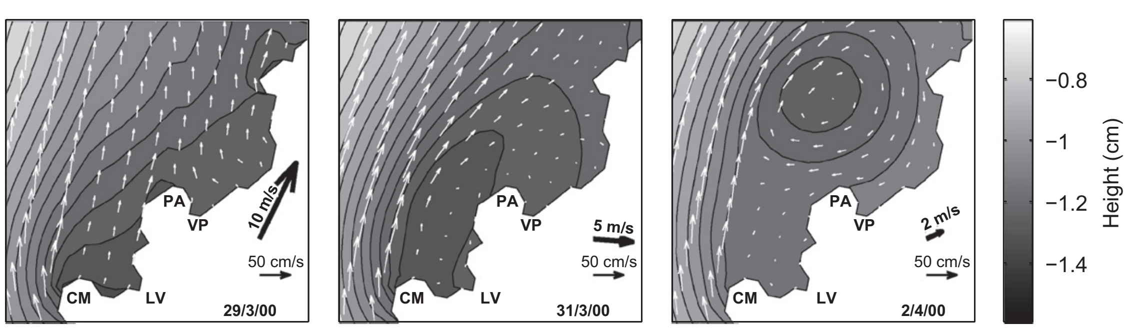

Fig. 8. Development of a topographic eddy in the lee of Curaumilla Point during the period March 29–April 2, 2000. Surface velocity is indicated by white vectors and anomalous surface elevation by the shading. The wind speed and direction are indicated by the thick arrow, while the thin arrow gives the scale for ocean velocity. Key locations are shown: Curaumilla Point (CM), Laguna Verde Bay (LV), Angeles Point (PA) and Valparaíso Bay (VP).

Topocalma Point was inferred to occur through an on-shore bottom boundary layer, driven by northwards acceleration of the CCC close to the headland, reinforced by flow curvature effects. These processes were also found to occur at Curaumilla Point, although in concert with the development of shallow vertical overturning flow within Laguna Verde Bay north of the headland. The combination of these mechanisms may explain the relatively high intensity of upwelling at Curaumilla compared to other nearby upwelling centres. In contrast, neither of these processes occurred strongly within Valparaíso Bay, despite its geometrical similarity to Laguna Verde Bay. Sheltering of the bay from upwelling-favourable winds was found to be important for explaining the observed SST difference between Valparaíso and Laguna Verde Bay.

A recirculating eddy originating in Valparaiso Bay was a robust feature of the simulations, often leaving the bay but persisting within the model domain for a number of weeks. This eddy has not been previously described in observational studies, although it is suggested in observations by Johnson et al. (1980). If found to occur regularly, this eddy may prove to have some biological importance in the area, providing a mechanism for the retention of larvae and nutrients.

Acknowledgements

This research was supported by an Andrew Mellon Foundation grant to S.A.N. and FONDAP-FONDECYT grant 15001-001 to the Center for Advanced Studies in Ecology and Biodiversity. Additional support was provided by Fondecyt grants #1070335 to S.A.N. and #11060077 to C.M.A. while writing this paper. We thank the anonymous reviewers for their comments.

References

Aiken, C.M., Moore, A.M., Middleton, J.H., 2003. Nonnormal perturbation growth in idealised island and headland wakes. Dynamics of Atmospheres and Oceans 37, 171–195.

Aiken, C.M., Navarrete, S.N., Castillo, M.I., Castilla, J.C., 2007. Along-shore larval dispersal kernels in a numerical ocean model of the central Chilean coast. Marine Ecology Progress Series 339, 13–24.

Alaee, M.J., Ivey, G., Pattiaratchi, C., 2004. Secondary circulation induced by flow curvature and Coriolis effects around headlands and islands. Ocean Dynamics 54, 27–38.

Blumberg, A.F., Mellor, G.L., 1987. A description of a three-dimensional coastal ocean circulation model. In: Heaps, N.S. (Ed.), Three-Dimensional Coastal Ocean Models. American Geophysical Union, pp. 1–16.

Castilla, J.C., Lagos, N.A., Guiñez, R., Largier, J.L., 2002. Embayments and nearshore retention of plankton: the Antofagasta Bay and other examples. In: Castilla, J.C., Largier, J.L. (Eds.), The Oceanography and Ecology of the Nearshore and Bays in Chile. Universidad Católica de Chile, Santiago, Chile.

Figueroa, D., Moffat, C., 2000. On the influence of topography in the induction of coastal upwelling along the Chilean coast. Geophysical Research Letters 27, 3905–3908.

Fonseca, T., 1989. An overview of the poleward undercurrent and upwelling along the Chilean coast. In: CNKM Neshyba, S.J., Smith, R.L., Barber, R.T. (Eds.), Polewards Flow Along Eastern Boundaries. Springer, New York, pp. 203–218.

Galperin, B., Kantha, L.H., Hassid, S., Rosati, A., 1988. A quasi-equilibrium turbulent energy model for geophysical flows. Journal of the Atmospheric Sciences 45, 55–62.

Graham, W.M., Largier, J.L., 1997. Upwelling shadows as nearshore retention sites: the example of Monterrey Bay. Continental Shelf Research 17, 509–532.

Halpin, P.M., Strub, P.T., Peterson, W.T., Baumgartner, T., 2004. An overview of interactions among oceanography, marine ecosystems, climatic and human disruptions along the eastern margins of the Pacific Ocean. Revista Chilena de Historia Natural 77, 371–409.

Hamrick, J.M., 1992. A three-dimensional environmental fluid dynamics computer code: theoretical and computational aspects. Virginia Institute of Marine Science, Special Report 317, 63pp.

Hamrick, J.M., Mills, W.B., 2000. Analysis of water temperatures in Conowingo Pond as influenced by the Peach Bottom atomic power plant thermal discharge. Environmental Science and Policy 3, s197–s209.

Johnson, W.R., Fonseca, T., Sievers, H., 1980. Upwelling in the Humboldt Coastal Current near Valparaiso, Chile. Journal of Marine Research 38 (1), 1–15.

Kalkwijk, J.P.T., Booij, R., 1986. Adaptation of secondary flow in nearly-horizontal flow. Journal of Hydraulic Research 24, 19–37.

Kaplan, D.M., Largier, J.L., Navarrete, S.A., Guiñez, R., Castilla, J.C., 2003. Large diurnal temperature fluctuations in the nearshore water column. Estuarine Coastal and Shelf Science 57, 385–398.

Lagos, N., Navarrete, S.A., Véliz, F., Masuero, A., Castilla, J.C., 2005. Meso-scale spatial variation in settlement and recruitment of intertidal barnacles along central Chile. Marine Ecology Progress Series 290, 165–178.

Largier, J.L., 2002. Linking oceanography and nearshore ecology: perspectives and challenges. In: Castilla, J.C., Largier, J.L. (Eds.), The Oceanography and Ecology of the Nearshore and Bays in Chile. Universidad Católica de Chile, Santiago, Chile.

Leth, O., Middleton, J.F., 2004. A mechanism for enhanced upwelling in central Chile: eddy advection. Journal of Geophysical Research 109, C12020.

Leth, O., Middleton, J.F., 2006. A numerical study of the upwelling circulation off central Chile: effects of remote ocean forcing. Journal of Geophysical Research 111, C12003.

Leth, O., Shaffer, G., 2001. A numerical study of the seasonal variability in the circulation of central Chile. Journal of Geophysical Research 106 (C10), 22,229–22,248.

Mellor, G.L., Yamada, T., 1982. Development of a turbulence closure model for geophysical fluid problems. Reviews of Geophysics and Space Physics 20, 851–875.

Mellor, G.L., Ezer, T., Oey, L.-Y., 1994. The pressure gradient conundrum of sigma coordinate ocean models. Journal of Atmospheric and Oceanic Technology 11, 1126–1134.

Mesias, J.M., Matano., R.P., Strub, P.T., 2001. A numerical study of the upwelling circulation off central Chile. Journal of Geophysical Research 106 (C9), 19611–19623.

Mesias, J.M., Matano., R.P., Strub, P.T., 2003. Dynamical analysis of the upwelling circulation of central Chile. Journal of Geophysical Research 108 (C3), 3085.

Middleton, J.F., Leth, O.K., 2004. Wind-forced setup of upwelling, geographical origins, and numerical models: the role of bottom drag. Journal of Geophysical Research C12019.

Narváez, D.A., Poulin, E., Leiva, G., Hernández, E., Castilla, J.C., Navarrete, S.A., 2004. Seasonal and spatial variation of nearshore hydrographic conditions in central Chile. Continental Shelf Research 24, 279–292.

Narváez, D.A., Navarrete, S.A., Largier, J., Vargas, C.A., 2006. Onshore advection of warm water and larval invertebrate settlement during relaxation of upwelling off central Chile. Marine Ecology Progress Series 309, 159–173.

Neshyba, S.J., Moores, C.N.K., Smith, R.L., Barber, R.T. (Eds.), 1989. Poleward flows along eastern ocean boundaries. Coastal and Estuarine Studies No. 34, Springer, New York, 1989, 374pp.

Oke, P.R., Middleton, J.H., 2000. Topographically induced upwelling off eastern Australia. Journal of Physical Oceanography 30, 512–531.

Oke, P.R., Allen, J.S., Miller, R.N., Egbert, G.D., Kosro, P.M., 2002. Assimilation of surface velocity data into a primitive equation coastal ocean model. Journal of Geophysical Research 107 (C9), 3122–3146.

Philander, S.G.H., Yoon, J.-H., 1982. Eastern boundary currents and coastal upwelling. Journal of Physical Oceanography 12, 862–879.

Piñones, A., Valle-Levinson, A., Narváez, D.A., Vargas, C.A., Navarrete, S.A., Yuras, G., Castilla, J.C., 2005. Wind-induced diurnal variability in river plume motion. Estuarine Coastal and Shelf Science 65, 513–525.

Pizarro, O., Hormazábal, S., González, A., Yáñez, E., 1994. Variabilidad del viento, el nivel del mar y la temperatura en la costa norte de Chile. Investigaciones Marinas (Valparaíso) 22, 85–101.

Poulin, E., Palma, A.T., Leiva, G., Narváez, D., Pacheco, R., Navarrete, S.A., Castilla, J.C., 2002. Avoiding offshore transport of competent larvae during upwelling events: the case of the gastropod *Concholepas concholepas* in central Chile. Limnology and Oceanography 47, 1248–1255.

Shchepetkin, A.F., McWilliams, J.C., 2003. A method for computing horizontal pressure-gradient force in an oceanic model with a non-aligned vertical coordinate. Journal of Geophysical Research 108 (C3), 3090.

Shen, J., Kuo, A.Y., 1999. Numerical investigation of an estuarine front and its associated topographic eddy. Journal of Waterway Port Coastal and Ocean Engineering 125, 127–135.

Sievers, H., Silva, N., 1979. Variación temporal de las condiciones oceanográficos frente a punta Curaumilla, Valparaíso, Chile (Mayo 1974–Abril 1975). Investigaciones Marinas (Valparaíso) 7, 2–30.

Silva, N., Valdenegro, A., 2003. Evolución de un evento de surgencia frente a punta Curaumilla, Valparaíso. Investigaciones Marinas (Valparaiso) 31 (2), 73–89.

Strub, P.T., Mesías, J.M., Montecino, V., Rutlland, J., Salinas, S., 1998. Coastal ocean circulation off Western South America. In: Robinson, B. (Ed.), The Sea, vol. 11. Wiley, pp. 273–313 (Chapter 10).

Suginohara, N., Kitamura, Y., 1984. Long-term coastal upwelling over a continental shelf-slope. Journal of Physical Oceanography 14, 1095–1104.

Valle-Levinson, A., Moraga-Opazo, J., 2006. Observations of bipolar residual circulation in two equatorward-facing semiarid bays. Continental Shelf Research 26, 179–193.

Vargas, C., Narváez, D., Piñones, A., Venegas, R.M., Navarrete, S.A., 2004. Internal tidal bore warm fronts and settlement of invertebrates in central Chile. Estuarine Coastal and Shelf Science 61, 603–612.

Wieters, E.A., Kaplan, D.M., Navarrete, S.A., Sotomayor, A., Largier, J., Nielsen, K.J., Véliz, F., 2003. Alongshore and temporal variability in chlorophyll a concentration in Chilean nearshore waters. Marine Ecology Progress Series 249, 93–105.

Yang, Z., Hamrick, J.M., 2005. Optimal control of salinity boundary condition in a tidal model using a variational inverse method. Estuarine, Coastal and Shelf Science 62, 13–24.